Elemental analysis of concrete via fast neutron transmission and scattering spectrometry

Tanya Hutton[1*], *Andy* Buffler[1], and *Mark* Alexander[2]

[1]Metrological and Applied Sciences University Research Unit (MeASURe), Department of Physics, University of Cape Town, South Africa.
[2]Concrete Materials and Structural Integrity Research Unit (CoMSIRU), Department of Civil Engineering, University of Cape Town, South Africa.

Abstract. We report on the development of neutron-based techniques to non-destructively measure the composition of concrete. Previous experimental studies demonstrated the viability of the unfolding technique to determine the ratio of water, sand and cement in well-characterised concrete samples from the transmitted neutron energy spectrum. In this work, we used MCNP6 simulations to demonstrate the extension of the technique to determine elemental compositions from transmitted, or scattered neutron energy spectra. In both cases, the simulated energy spectra provided a reliable method to unfold the composition of samples with known elemental ratios. The precision of the technique was limited by the statistical uncertainties of the simulated spectra, particularly for the case of scattered neutrons. The accuracy of the technique was heavily dependent on the uniqueness of each of the elemental responses, and reasonable prior knowledge of the composition. Given the promising results at this stage, future developments will include the addition of further elements to the response matrix, and experimental verification.

1 Introduction

Hydrogen-rich materials offer excellent neutron shielding, and concrete is widely used in nuclear facilities due to its structural strength, low cost, low activation and low maintenance requirements. The types of concrete used in nuclear installations are subject to a series of codes and standards, such as ACI 318, ACI 349 and ACI 359, which apply to concrete in nuclear power plants though these are subject to ongoing research and development [1]. The nuclear regulator for the region is then responsible for ensuring compliance between the regulatory radiation safety standards and the physical installation at all stages of the life-cycle. In this project we aim to develop and characterize a new experimental research and testing facility that will be used to facilitate investigations requiring radiation-based characterization of concrete (and other materials) for the nuclear industry. Of particular interest is the ability to non-destructively determine the water content in concrete, which is a known problem for ageing nuclear facilities as a reduction in hydrogen content results in a

* Corresponding author: tanya.hutton@uct.ac.za

reduction in the effectiveness as a neutron shield [2]. In the case of radiation transport simulations of nuclear facilities, poor knowledge of the concrete composition, in particular the hydrogen content, can cause significant discrepancies between measured and simulated neutron spectra and associated dose rates [3].

Materials analysis utilising fast neutrons is advantageous in this context as fast neutrons are non-invasive, highly penetrating, sensitive to low mass nuclei and produce characteristic secondary radiation for each nuclide. In fast neutron transmission measurements, a beam of fast neutrons is incident upon a sample and the fluence, and potentially energy distribution, of the exiting neutrons are measured. Information concerning the neutrons which have interacted in the sample can be obtained if the energy dependent fluence entering the sample is known. This technique has been applied in many contexts, such as the detection of explosives [4] using a ns-pulsed neutron beam, or scanning for illicit materials in cargo by considering the ratio of neutron and gamma ray attenuation coefficients [5].

In previous studies at the University of Cape Town, the water content in concrete has been experimentally measured through spectral unfolding [6]. Energy dependent response functions were measured for water, sand and cement, and were successfully used to unfold the composition of a concrete sample within 5% of the known values. However, there may be instances where the composite ingredients are not available, and the material composition is often location specific. For example, sand mined from coastal regions will contain variable proportions of calcium carbonate relative to sand obtained from an inland mine [7]. In this work we investigate the use of fast neutron transmission and scattering spectrometry to characterise the elemental composition of materials through Monte Carlo radiation transport simulations.

2 Approach

There are three main signatures used for the analysis of materials in bulk using fast neutrons: transmitted neutrons; elastically and inelastically scattered neutrons; and gamma rays produced from neutron-induced reactions. As neutrons interact with atomic nuclei in distinctive, energy dependent ways, the signatures produced by each element are also distinct. If then, measurements of these signatures are made for a composite material, the elemental composition can be determined from these signatures according to Equation 1, where S_j is the measured signature for the composite sample in channel j, R_{jk} is the response function associated with element, k in channel j, and p_k is the projected number density of element, k.

$$S_j = \sum_k R_{jk} p_k \tag{1}$$

The elemental composition can then be de-convolved from the measured signatures through a least-squares minimisation procedure. To develop elemental response functions and verify the procedure, Monte Carlo radiation transport simulations of a highly simplified scenario were undertaken with MCNP6.1 [8] for the exemplar case of sand, a key constituent of concrete.

2.1 Simulation details

The simulations comprised of a 0.8 cm diameter pencil beam of fast neutrons, with a uniform energy distribution between 1.0 MeV and 14.0 MeV, incident upon elementally, and isotopically, pure samples of ^{1}H, ^{16}O, ^{28}Si, and ^{40}Ca. All neutron reaction cross sections used in these simulations were from the ENDF/B-VII.1 evaluation [9]. The cylindrical sample dimensions were defined as 1.0 cm along the beam axis, with a radius of 1.0 cm, with a fixed atom density of 1.0 $b^{-1}\,cm^{-1}$. Four spherical detector regions with radii of 1.0 cm were located at 0°, 45°, 90° and 135° relative to the beam axis, at a distance of 50.0 cm from the centre of the sample. These detector regions were used to determine the average energy dependent neutron flux using a track-length estimator (F4 tally). In this instance no additional variance reduction was implemented, and each simulation was run such that the statistical uncertainties on each bin were below 10 %. These simulations are highly idealised in terms of the incident neutron spectrum and sample properties for demonstration purposes. To realise this process experimentally, a broad spectrum neutron source such as ^{241}Am^{9}Be, and variable sample properties, could be used with appropriate normalisation.

2.2 Construction of response functions

Simulations of the elemental samples were used to develop the response functions required for the unfolding process. The scattered neutron spectra (45° - 135°) provide information on the neutrons which have interacted within the sample, so these can be directly used as the elemental response R_{jk} in this instance as described in Equation 1.

However, in the case of the transmitted neutron energy spectrum, this only provides information on the neutrons which have not interacted within the sample and requires further manipulation to be utilised as a response. Here we use the effective removal cross section [10], Σ_{jk}^{R}, calculated according to Equation 2, where ϕ_{jk} is the transmitted neutron flux in energy bin j for element k and sample thickness t, and ϕ_j^0 is the incident neutron flux in energy bin j. For composite materials, the effective removal cross section Σ_j^R is a linear combination of it constituent elements according to Equation 3, where p_k is the projected number density of the constituent element k, with density ρ_k.

$$\Sigma_{jk}^{\mathrm{R}} = -\ln\left(\frac{\phi_{jk}}{\phi_j^0}\right)\frac{1}{t} \tag{2}$$

$$\Sigma_{\mathrm{j}}^{\mathrm{R}}/\rho = \sum_k p_k(\Sigma_{jk}^R/\rho_k) \tag{3}$$

2.3 Unfolding of elemental composition of known materials

In order to determine the relative amounts of each element within a composite material, an unfolding procedure was utilised, in this instance the multi-channel unfolding programs GRAVEL and MAXED which form part of the UMG-33 software package [11].

To verify the unfolding procedure, simple combinations of hydrogen, oxygen, silicon and calcium were simulated, as given in Table 1, with the same geometry as used previously. The sand analogue used in these simulations is loosely based on the composition obtained from XRF analyses of real samples [6]. The simulated response functions for the elemental

samples were used to deconvolve the ratios of the different elements in the composite media from the transmitted and scattered signatures. A two-step unfolding process was implemented, first using GRAVEL, which is based on the SAND-II algorithm, and produces a solution spectrum through least-squares minimisation. As the starting point for the unfolding process, equal ratios of all elements were assumed, effectively representing the worst case scenario with regards to prior knowledge of the composition. The solution ratios produced by GRAVEL were then used as *a priori* information for unfolding with MAXED, which uses a maximum entropy approach, and allows for the propagation of uncertainties.

Table 1. Composite sample details.

Sample	ρ (g cm^{-3})
H_2O	1.0
SiO_2	2.7
CaO	3.3
Sand 1:8:1 (H_2O:SiO_2:CaO)	1.5

3 Results & Analysis

Each elemental simulation was run with a variable number of particle histories in order to achieve convergence, and comparable statistics for each of the simulated signatures. Figure 1 shows the spatial distribution of neutrons for (a) hydrogen and (b) silicon targets. As expected, the scattered neutron field is more isotropic for hydrogen relative to the forward biased distribution for silicon.

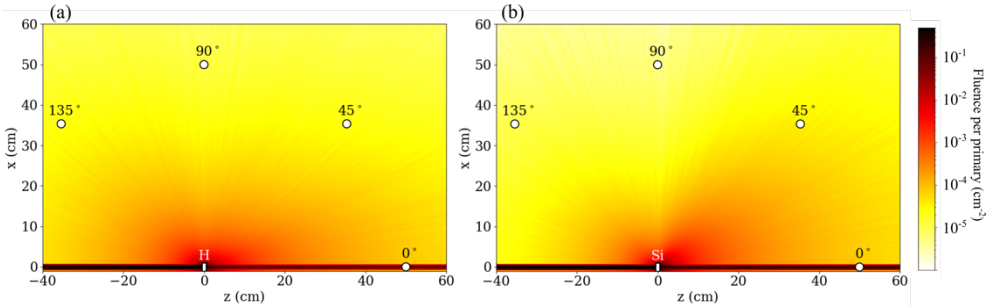

Fig. 1. Total neutron fluence over the simulated geometry for a broad spectrum neutron beam along the z-axis, incident on targets comprised of (a) hydrogen and (b) silicon respectively. Detector regions are indicated with the white circles.

3.1 Construction of response functions

Within each of the detector regions, the energy dependent neutron fluence was scored, and can be seen in Figure 2. For clarity, statistical uncertainties have been excluded from the figures. For the transmitted (0°) spectra, statistical uncertainties were below 1 %, and between

1 % and 10 % for the scattered spectra (45°-135°). Unique features in the simulated spectra, such as the smoothly varying distribution for hydrogen, and the enhancement in the 2-3 MeV region for oxygen, start to become apparent and are directly related to the underlying interaction cross sections.

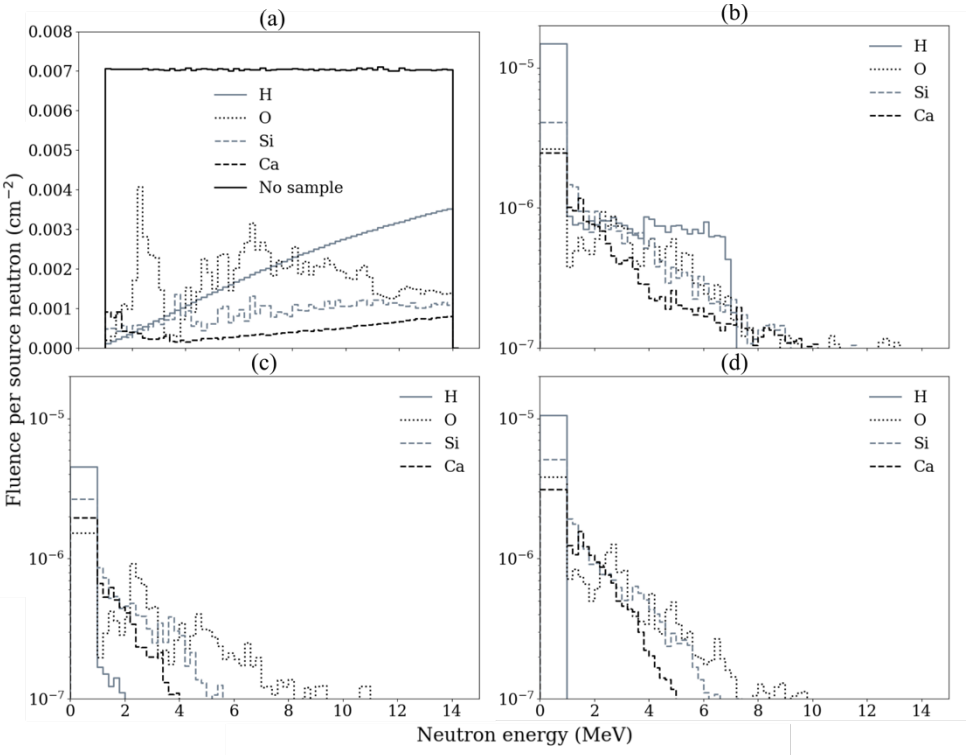

Fig. 2. Energy dependent neutron fluence, per source neutron, for elemental samples in the detector regions at (a) 0°, (b) 45°, (c) 90° and (d) 135° relative to the beam axis. Note that a log fluence scale is used for the scattered spectra (b-d).

From the simulated energy spectra the elemental response functions are constructed, utilising the effective removal cross section for the transmission simulations according to Equation 2, and selected energy ranges for the scattered spectra. The statistical uncertainties associated with the response functions were accounted for through an appropriate choice of precision. The elemental response functions were compiled into a response matrix with a format compatible with the UMG unfolding package, and can be seen in Figure 3.

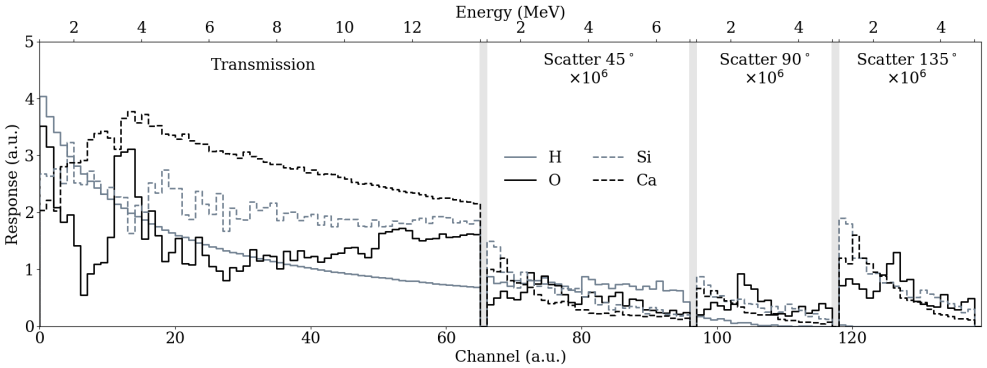

Fig. 3. Response functions constructed for elemental samples of hydrogen, oxygen, silicon and calcium. Effective removal cross sections are used between 1.0 MeV and 14.0 MeV for the transmission component. The scattered components consist of the simulated energy spectra between 1.0 MeV and 7.0 MeV for 45°, and 1.0 MeV and 5.0 MeV for 90° and 135°. For convenience the scattered fluence spectra have been multiplied by a factor of 10^6.

3.2 Unfolding of elemental composition of known materials

Transmitted and scattered energy spectra were obtained for the composite samples detailed in Table 1, and the simulated signatures shown in Figure 4 were constructed by the same process used to develop the elemental responses. The ratios of H, O, Si and Ca were unfolded from either the transmitted, or scattered signatures.

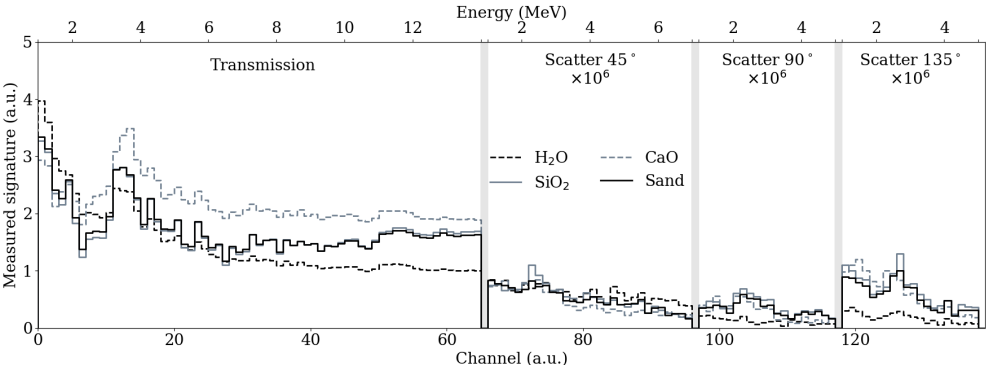

Fig. 4. Transmitted and scattered neutron signatures for the composite materials H_2O, SiO_2, CaO and sand as defined in Table 1. Statistical uncertainties have been excluded for clarity, but are below 1 % for the transmission signatures, and below 10 % for the scattered signatures.

For the exemplar case of H_2O, the simulated and re-folded signatures are shown in Figure 5. For the transmitted neutrons there is excellent agreement between the two over the full energy range with little deviation. In the case of scattered neutrons the quality of the calculated signature is limited by the poor statistics associated with the simulated signatures and a non-optimised energy binning structure, though the overall agreement is considered acceptable across the three angles used.

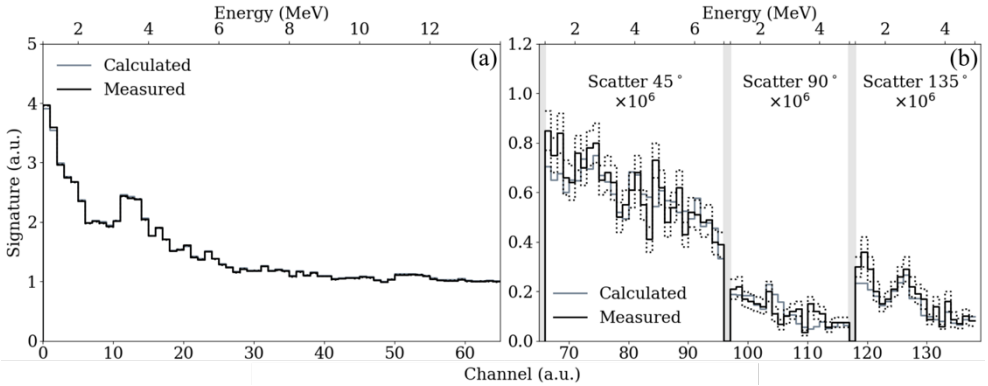

Fig. 5. Simulated signatures for (a) transmitted (0°) neutrons, and (b) scattered neutrons (45°-135°), shown together with the refolded signatures obtained using the MAXED package. Statistical uncertainties on the simulated signatures are indicated with the dotted lines.

The resulting elemental ratios obtained from the unfolding process of the composite materials are shown in Figure 6. In all but a few cases, the resulting elemental composition was in agreement with the known values. The most notable instance is the minor misclassification of calcium in CaO as silicon in the transmitted analysis, which suggests there is insufficient uniqueness between the two signatures with the current structure. This could be mitigated through a more appropriate choice of the initial ratios, but requires some prior knowledge of the material. For H_2O and sand, the ratio of hydrogen was reproduced from the unfolding analyses within the tolerance of the statistical uncertainties. The difference between the expected and unfolded elemental ratios for sand are presented in Table 2 with their statistical uncertainties.

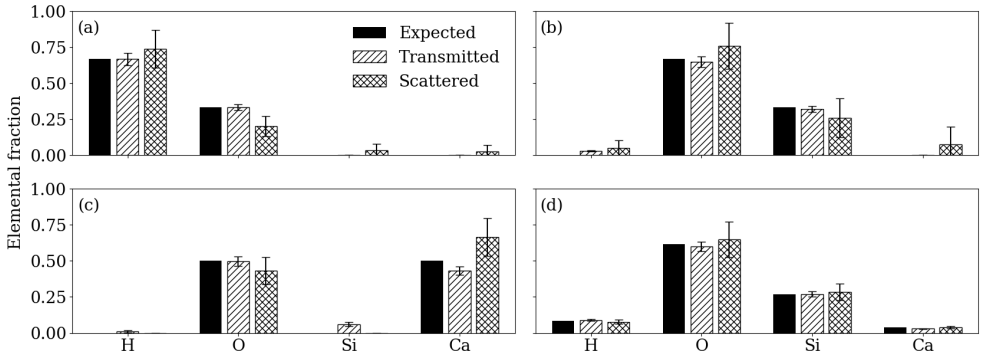

Fig. 6. Elemental fractions of H, O, Si and Ca unfolded from either the transmitted or scattered signatures for (a) H_2O, (b) SiO_2, (c) CaO, and (d) sand. In each case, the known ratio (black) is included for comparison.

Table 2. Difference between expected and unfolded elemental ratios for transmitted (Δ_T) and scattered (Δ_S) analyses for the case of sand.

	Δ_T (%)	Δ_S (%)
H	0.50 ± 0.55	-1.0 ± 1.0
O	-0.4 ± 3.1	1.2 ± 8.7
Si	0.5 ± 1.4	0.4 ± 4.0
Ca	-0.83 ± 0.27	0.05 ± 0.50

4 Conclusion

In this work we aimed to demonstrate the use of spectrum unfolding as a means to determine the elemental composition of materials. Monte Carlo simulations were used to produce energy dependent elemental response functions for transmitted and scattered neutrons. Elemental ratios were unfolded from simulated signatures for a series of composite materials, where the truth values were known. Practically, transmitted neutron spectroscopy is the preferred mode due to the higher detection rates, though this requires knowledge of the incident spectrum. Scattered neutron spectroscopy, while limited by potentially poor statistics, provides a viable alternative in instances where transmission is not possible, for example, if no safe access is possible behind a thick radiation shield. In all instances, the reliability of the unfolded elemental ratios is dependent on the quality and uniqueness of the response functions. Future developments on this project consist of the experimental verification of the response functions as far as reasonably possible, and the inclusion of additional elements to broaden the range of potential applications.

We thank the National Nuclear Regular (South Africa) through the Centre for Nuclear Safety and Security for their support of this project (CNSS0117-E5-UCT)

References

1. C. Ferraris, *Concrete Codes and Standards for Nuclear Power Plants: Recommendations for Future Development*, ANSI publications (2011)
2. E.G. Peterson, *Shielding Properties of Ordinary Concrete as a Function of Temperature*, USAEC, Report HW-65572 (1960)
3. M. Petit, Nucl. Sci. Eng., **195**:8, 846 (2021)
4. J.C. Overley, Appl. Radiat. Isot. **36:**3 185 (1985)
5. J.E. Eberhardt, S. Rainey, R.J. Stevens, B.D. Sowerby, J.R.Tickner, Appl. Radiat. Isot., **63**:2, 179 (2005)
6. A. Buffler, T. Hutton, T. Leadbeater, Int. J. Mod. Phys., **50**, 2060015 (2020)
7. B. Walker, *Fine Aggregate Resources in the Greater Cape Town Area*, Master's thesis, University of Cape Town (2013)
8. T. Goorley, M. James, T. Booth, F. Brown, J. Bull, L. J. Cox, J. Durkee, J. Elson, M. Fensin, R. A. Forster, J. Hendricks, H. G. Hughes, R. Johns, B. Kiedrowski, R. Martz, S. Mashnik, G. McKinney, D. Pelowitz, R. Prael, J. Sweezy, L. Waters, T. Wilcox, T. Zukaitis, Nucl. Tech., **180**, 298 (2012)
9. M.B. Chadwick, M. Herman, P. Obložinský, M.E. Dunn, Y. Danon, A.C. Kahler, D.L. Smith, B. Pritychenko, G. Arbanas, R. Arcilla, R. Brewer, D.A. Brown, R. Capote, A.D. Carlson, Y.S. Cho, H. Derrien, K. Guber, G.M. Hale, S. Hoblit, S. Holloway, T.D. Johnson, T. Kawano, B.C. Kiedrowski, H. Kim, S. Kunieda, N.M. Larson, L. Leal, J.P. Lestone, R.C. Little, E.A. McCutchan, R.E. MacFarlane, M. MacInnes, C.M. Mattoon, R.D. McKnight, S.F. Mughabghab, G.P.A. Nobre, G. Palmiotti, A. Palumbo, M.T. Pigni, V.G. Pronyaev, R.O. Sayer, A.A. Sonzogni, N.C. Summers, P. Talou, I.J. Thompson, A. Trkov, R.L. Vogt, S.C. van der Marck, A. Wallner, M.C. White, D. Wiarda, P.G. Young, Nucl. Dat. Sh., **112**:12, 2887 (2011)
10. R.D. Albert, T.A. Welton, *A simplified theory of neutron attenuation and its application to reactor shield design*, USAEC, Report WAPD-15 (1950)
11. M. Reginatto, Radiat. Meas., **45**, 1323 (2010)